

UNCLASSIFIED

AD 296 288

*Reproduced
by the*

**ARMED SERVICES TECHNICAL INFORMATION AGENCY
ARLINGTON HALL STATION
ARLINGTON 12, VIRGINIA**



UNCLASSIFIED

NOTICE: When government or other drawings, specifications or other data are used for any purpose other than in connection with a definitely related government procurement operation, the U. S. Government thereby incurs no responsibility, nor any obligation whatsoever; and the fact that the Government may have formulated, furnished, or in any way supplied the said drawings, specifications, or other data is not to be regarded by implication or otherwise as in any manner licensing the holder or any other person or corporation, or conveying any rights or permission to manufacture, use or sell any patented invention that may in any way be related thereto.

65-2-4

CAVALRY
AS AD No. 296288

RADC-TDR-62-633

Date October 17, 1962

Copy No. 42

FAILURE MECHANISMS IN CERAMIC DIELECTRICS

D. Berlincourt

Electronic Research Division
Clevite Corporation
Cleveland, Ohio

Quarterly Technical Note No. 3

Contract No. AF 30(602)-2594

RECEIVED
OCT 18 1962
RADC-TDR-62-633

296 288

Prepared for
Rome Air Development Center
Air Force Systems Command
United States Air Force
Griffiss Air Force Base
New York

ASTIA NOTICE

Qualified requestors may obtain copies of this report from the Armed Services Technical Information Agency, Arlington Hall Station, Arlington 12, Virginia. ASTIA Services for the Department of Defense Contractors are available through the "Field of Interest Register" on a "need-to-know" certified by the cognizant military agency of their project or contract.

PATENT NOTICE

When Government drawings, specifications, or other data are used for any purpose other than in connection with a definitely related Government procurement operation, the United States Government thereby incurs no responsibility nor any obligation whatsoever and the fact that the Government may have formulated, furnished, or in any way supplied the said drawings, specifications or other data is not to be regarded by implication or otherwise as in any manner licensing the holder or any other person or corporation, or conveying any rights or permission to manufacture, use, or sell any patented invention that may in any way be related thereto.

FOREWORD

This report was prepared for Rome Air Development Center, Air Force Systems Command, United States Air Force under Contract No. AF 30(602)-2594, Project No. 5519, Task No. 45155.

Robert Gerson directed this research work in the period preceding September 1, 1962, when he assumed a new position as Professor of Physics at University of Missouri School of Mines and Metallurgy. The research work has since been directed by Don Berlincourt, who has had the assistance of F. J. Scholz, J. M. Peterson, and W. M. Szczecinski. The reader is referred also to the first and second quarterly technical notes of this series, RADC-TDR-62-267 and RADC-TDR-62-406.

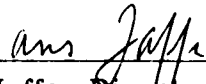
ABSTRACT

In a continuing effort to establish mechanisms of failure in ceramic dielectrics, this program has reached the point where significant results are being obtained in the degradation studies. In these studies ceramic specimens were subjected to high dc field (significantly lower than the dielectric strength), and the volume resistivity was measured as a function of time for over 100 hours. The changes of dielectric constant and $\tan \delta$ as a result of the dc field exposure were also determined.

Attempts were made to correlate results of these degradation studies with composition, grain size, and with n- or p-type off-valency additives. The zirconates as a class suffered far less degradation than the titanates. In fact all zirconates tested so far have had increasing volume resistivity with exposure time for the period of these tests. Preliminary results indicate that n-type additives are beneficial, p-type deleterious. This may, however, be dependent on the base material. No correlation with grain size has been noted so far.

Relatively little ceramic preparation was undertaken during this quarter. Permittivity-temperature data are, however, shown for several new compositions.

Approved



Hans Jaffe, Director
Electronic Research

TABLE OF CONTENTS

| SECTION | | PAGE |
|---------|---------------------------------|------|
| I | DEGRADATION STUDIES | 1 |
| II | PERMITTIVITY-TEMPERATURE CURVES | 17 |
| III | FUTURE PLANS | 17 |

LIST OF TABLES AND FIGURES

| | | |
|------------|--|----|
| Table I. | Classification of Compositions with Respect to Their Behavior During Degradation Tests | 4 |
| Figure 1. | Life Test Circuit | 3 |
| Figure 2. | Life Test Jig | 5 |
| Figure 3. | Resistivity vs. Elapsed Time; Average Curve for Three Samples at 10 kV/cm, 230°C; PbZrO_3 | 6 |
| Figure 4. | Resistivity vs. Elapsed Time; Average Curve for Two Samples at 10 kV/cm, 230°C; $(\text{PbZrO}_3)_{0.98} + (\text{PbNb}_2\text{O}_6)_{0.02}$ | 7 |
| Figure 5. | Resistivity vs. Elapsed Time at 10 kV/cm, 230°C $(\text{Pb}_{0.60}\text{Ba}_{0.40}\text{ZrO}_3)_{0.99} + (\text{PbNb}_2\text{O}_6)_{0.01}$ | 8 |
| Figure 6. | Resistivity vs. Elapsed Time at 10 kV/cm, 230°C $(\text{Pb}_{0.50}\text{Sr}_{0.50}\text{ZrO}_3)_{0.99} + (\text{PbNb}_2\text{O}_6)_{0.01}$ | 9 |
| Figure 7. | Resistivity vs. Elapsed Time; Average Curve for Three Samples at 10 kV/cm, 230°C; $(\text{Pb}_{0.30}\text{Sr}_{0.70}\text{TiO}_3)_{0.99} + (\text{PbNb}_2\text{O}_6)_{0.01}$ | 10 |
| Figure 8. | Resistivity vs. Elapsed Time; Average Curve for Three Samples at 10 kV/cm, 230°C; $\text{Pb}_{0.30}\text{Sr}_{0.70}\text{TiO}_3$ | 11 |
| Figure 9. | Resistivity vs. Elapsed Time; Average Curve for Three Samples at 10 kV/cm, 230°C; $(\text{Pb}_{0.50}\text{Sr}_{0.50}\text{TiO}_3)_{0.99} + (\text{PbNb}_2\text{O}_6)_{0.01}$ | 12 |
| Figure 10. | Resistivity vs. Elapsed Time at 10 kV/cm, 230°C, $(\text{Pb}_{0.30}\text{Sr}_{0.70}\text{TiO}_3)_{0.99} + (\text{Pb}_2\text{Sc}_2\text{O}_5)_{0.01}$ | 13 |
| Figure 11. | ϵ/ϵ_0 vs. Temperature for (A) $\text{Ba}_{0.55}\text{Sr}_{0.45}\text{TiO}_3$ (B) $(\text{Ba}_{0.55}\text{Sr}_{0.45}\text{TiO}_3)_{0.99} + (\text{Ba}_2\text{Sc}_2\text{O}_5)_{0.01}$ | 18 |
| Figure 12. | ϵ/ϵ_0 vs. Temperature for (A) $\text{Ba}_{0.85}\text{Sr}_{0.15}\text{TiO}_3$, (B) $(\text{Ba}_{0.55}\text{Sr}_{0.45}\text{TiO}_3)_{0.99} + (\text{BaNb}_2\text{O}_6)_{0.01}$ | 19 |
| Figure 13. | ϵ/ϵ_0 vs. Temperature for $(\text{PbZrO}_3)_{0.98} + (\text{Pb}_2\text{Sc}_2\text{O}_5)_{0.02}$ | 20 |

I. DEGRADATION STUDIES

In work reported previously under this contract several perovskite compositions were prepared. With perovskite materials (ABO_3) the A-position may be filled by a positive ion of large ionic radius, the B-position by a positive ion whose radius is 30 to 40% smaller. Pb^{2+} , Ba^{2+} , and Sr^{2+} are A-position elements, and Ti^{4+} and Zr^{4+} are B-position elements used in this work. The lead ion provides high polarizability, hence leads in general to stronger ferroelectric interaction than Sr^{2+} or Ba^{2+} . The higher volatility of lead at the firing temperature provides more ready approach to chemical equilibrium. Nb^{5+} and Sc^{3+} , which from size considerations fit into the B-position, have been used to modify the basic materials. Nb^{5+} acts as an electron donor, Sc^{3+} as an acceptor. If the unmodified ceramic is p-type, as is usually the case, the donor tends to raise the volume resistivity by a compensation process. Similar considerations hold for n-type base ceramic doped with an acceptor. The addition of Nb^{5+} or Sc^{3+} profoundly affects the dielectric properties of the base materials as well, as has been noted for off-valency additions to piezoelectric lead titanate zirconate ceramics, ^(1, 2, 3) and in previous reports under this contract.

In work reported here an attempt is made to correlate results of degradation studies with A- and B-position elements, and n- and p-type additives. Heretofore in this work it has been noted that Nb^{5+} (n-type doping) substantially increases volume resistivity for all lead-containing ceramics with the possible exception of lead zirconate. In general the volume resistivities of undoped zirconates are substantially higher than for the undoped titanates, presumably because Ti^{4+} is more easily reduced than is Zr^{4+} . Any attempt to correlate results of degradation studies with chemical composition must be made with the effects of composition on volume resistivity in mind.

The primary interest in this work is degradation which occurs upon exposure to relatively high electric stress substantially below the dielectric strength.

(1) F. Kulcsar, J. Am. Cer. Soc. 42, 343 (1959).

(2) R. Gerson, J. Appl. Phys. 31, 188 (1960).

(3) H. Jaffe, Proc. Inst. Elect. Eng. 109, Part B., Supp. 22, 351 (1962).

This type of degradation is primarily electrochemical, and results in reduced volume resistivity and permittivity (hence reduced time constant, $\rho\epsilon$). The rate of degradation of commercial capacitors operating at rated electric stress is slow enough to make laboratory testing inconvenient. The usual approach under these circumstances is to accelerate the test either by increasing the electric stress or by raising the temperature. These deviations from normal conditions may, however, introduce new deterioration mechanisms. The approach chosen in this work is to make tests at one or several elevated temperatures in the hope that results may be extrapolated to the design temperature. An attempt will be made to correlate results of the degradation tests with other properties, such as dielectric strength, volume resistivity, and grain size.

Test specimens as fired are about 3/4" in diameter by 0.040 to 0.060" thick. For degradation studies the specimens are lapped to 0.010" thickness in two stages of lapping with silicon carbide grit. Then discs of 6 mm diameter are cut from the larger discs with an ultrasonic impact grinder. Gold electrodes about 4 mm in diameter are then applied. The electrode material is duPont 3N gold paste* baked on at 600°C for about one hour. Gold is thought to be a superior material in comparison, for instance, with silver, since electrochemical effects involving the electrode may be an important factor in these tests.

The circuit used in the degradation studies is shown in Figure 1. The power supply is the Lambda Model 71 Regulated Power Supply. R_2 is a two-watt potentiometer whose resistance is about 0.5 megohm. The power dissipated in R_2 is therefore less than 0.5 watts with 500 volts input. R_2 is set so that the tapped output is 250 volts, thus providing an electric field of 10 kv/cm across the test specimen. R_1 is a current-metering resistance for determination of the current through the test specimen. Its value is chosen such that the voltage drop across it is less than 2.5 volts. With this arrangement the power supply would not be overloaded in case the test specimen should suffer dielectric failure, and in such case the power dissipation in the upper half of R_2 would reach only one watt.

* E. I. duPont de Nemours Co., Wilmington 98, Delaware.

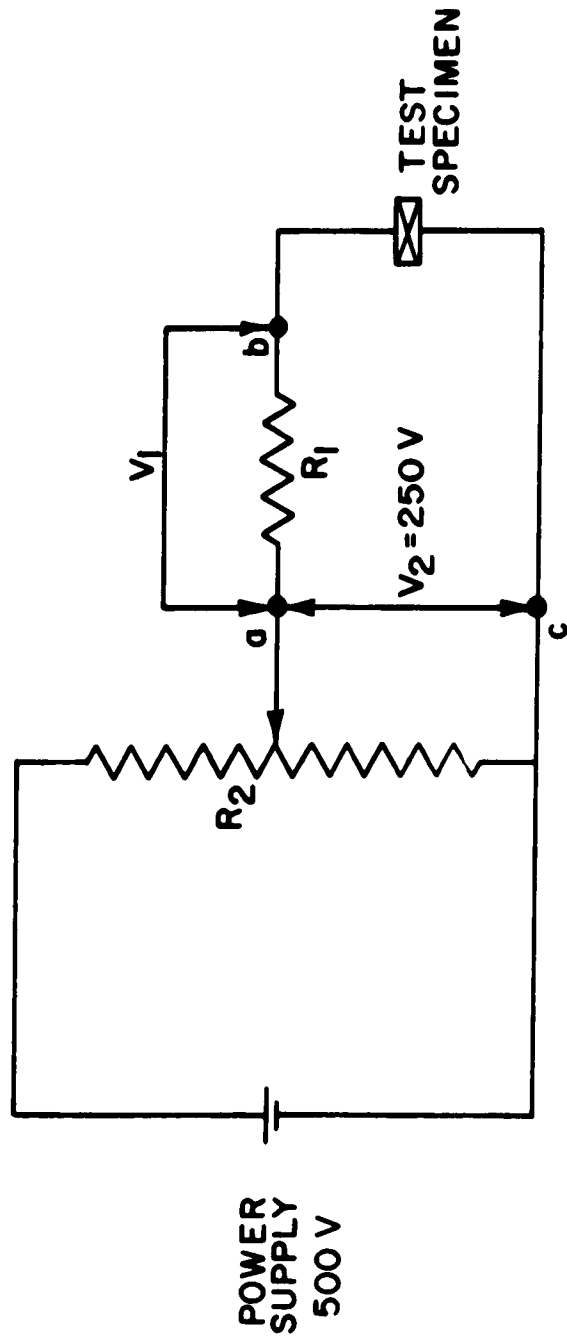


FIGURE 1.
LIFE TEST CIRCUIT

The resistance of the test specimen R_{TS} is given by:

$$R_{TS} = R_1 \frac{V_2 - V_1}{V_1} \sim R_1 \frac{V_2}{V_1}$$

V_1 and V_2 are measured with Keithley Model 610 and 210 electrometers respectively. In nearly all instances the point (a) is grounded.

Potentiometer R_2 and metering resistance R_1 are mounted on an insulated panel. The test specimen is placed in a furnace, the Hevi-Duty type 051. Points a and b are accessible on the lucite panel.

A diagram of the experimental arrangement for holding test specimens in the furnace is shown in Figure 2. Electrical connection to the test specimens is made via the silver rods A. The lower ends of these rods are coated with duPont 3N gold paste to prevent formation of oxide layers. The upper ends of the rods are connected to the respective resistances R_1 by alligator clipped fine wire (phonograph pickup arm cable). The plates B_1 and B_2 were fabricated from boron nitride in order to prevent leakage currents between the silver rods A. The thermal insulation inside the furnace door was removed around the alumina tubes F, also to prevent leakage currents. The sole function of the alumina connecting rods E is to support plate H, which holds the test specimens. In one experimental set-up plate H is silver and is coated with duPont 3N gold paste. In the other, presently being completed, plate H is gold with a stainless steel plate underneath for support.

The volume resistivity at 230°C with an electric field of 10 kv/cm maintained is shown as a function of the log of time in Figures 3 through 10 and in Figure 24 of Quarterly Technical Note No. 2. The various compositions may be classified in three categories: a) those whose volume resistivity increased with time during the period of these tests (generally 100 to 250 hours), b) those whose volume resistivity was virtually unchanged during the period of the tests, and c) those whose volume resistivity decreased during the period of the tests. Table I classifies the various compositions with respect to their behavior, and gives the

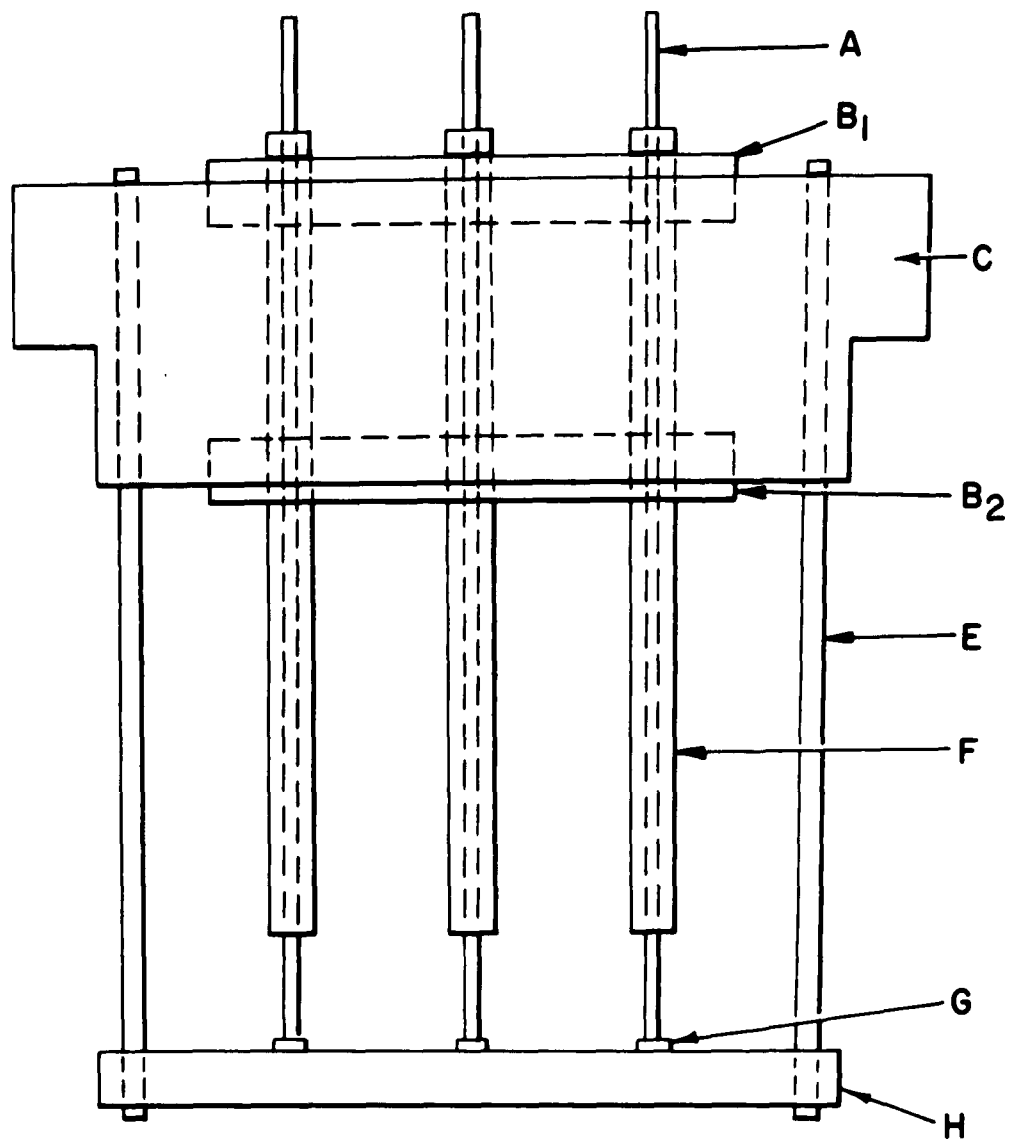


FIGURE 2.
LIFE TEST JIG

FIGURE 3.
RESISTIVITY VS. ELAPSED TIME
AVERAGE CURVE FOR 3 SAMPLES
10 KV/CM 230°C
PbZrO₃

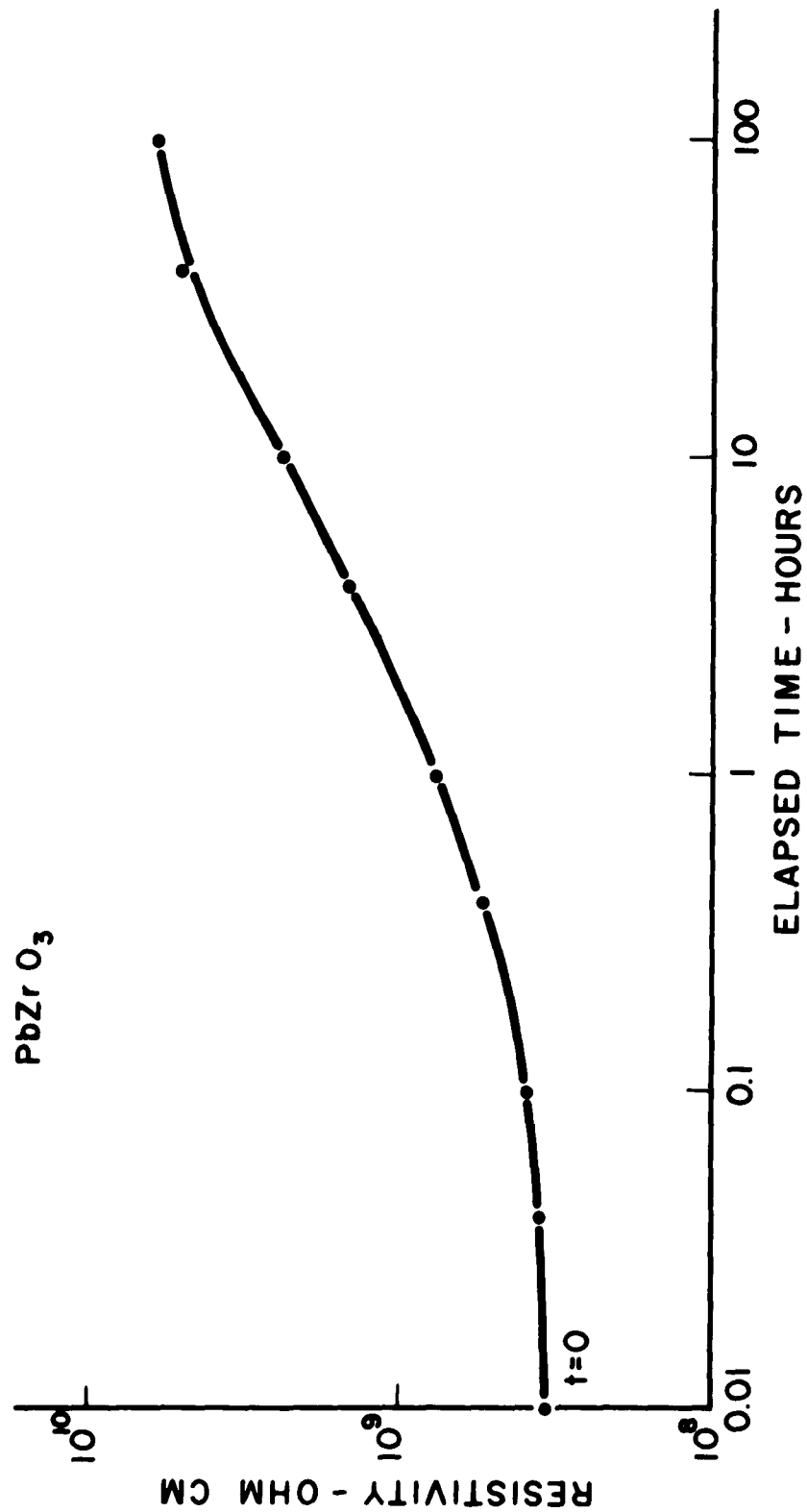


FIGURE 4.
RESISTIVITY VS. ELAPSED TIME
AVERAGE CURVE FOR 2 SAMPLES
10 KV/CM 230°C
 $(\text{PbZrO}_3)_{0.98} + (\text{PbNb}_2\text{O}_6)_{0.02}$

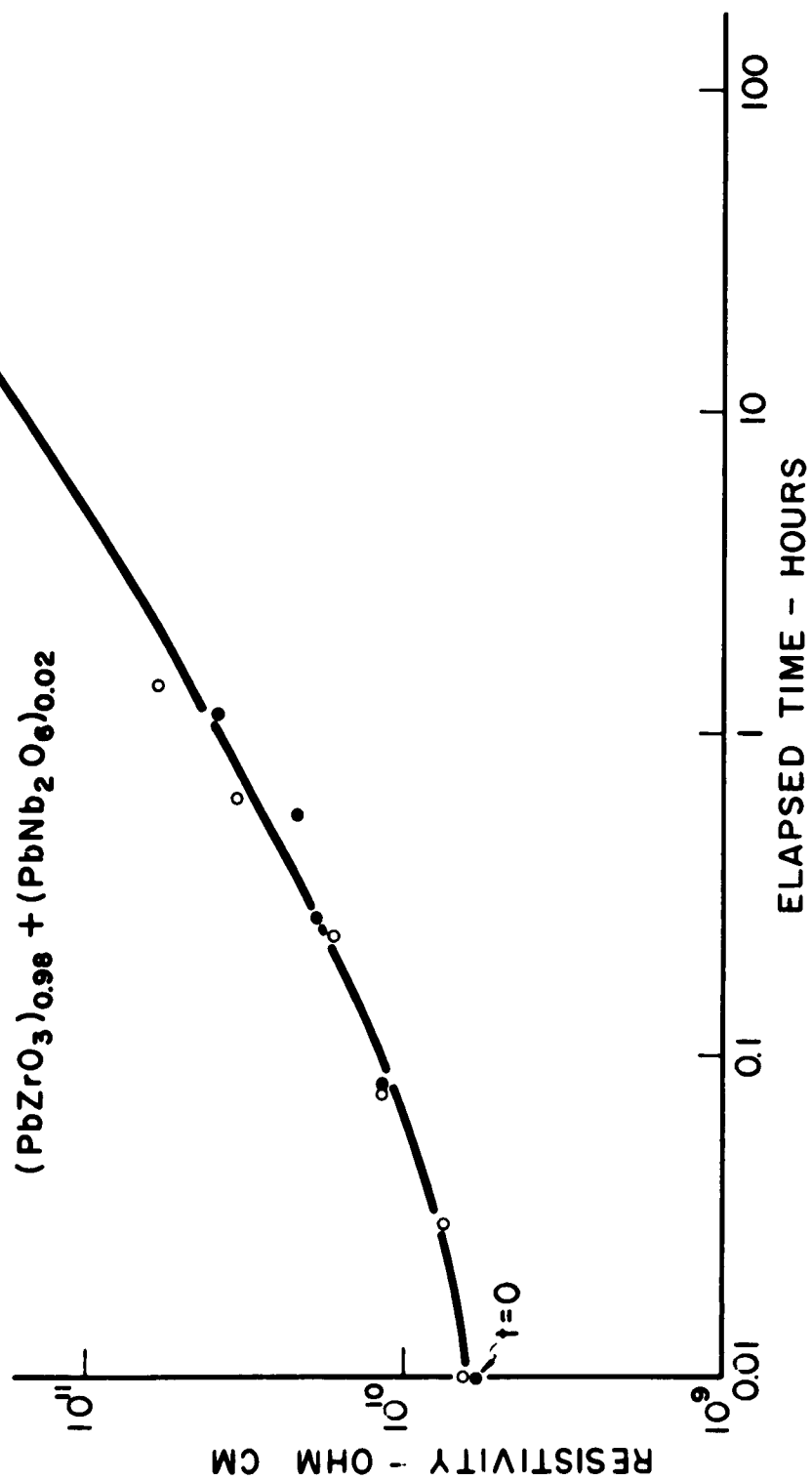


FIGURE 5.
RESISTIVITY VS. ELAPSED TIME
10 KV/CM 230°C
 $(\text{Pb}_{0.60}\text{Ba}_{0.40}\text{ZrC}_3)_{0.99} + (\text{PbNb}_2\text{O}_6)_{0.01}$

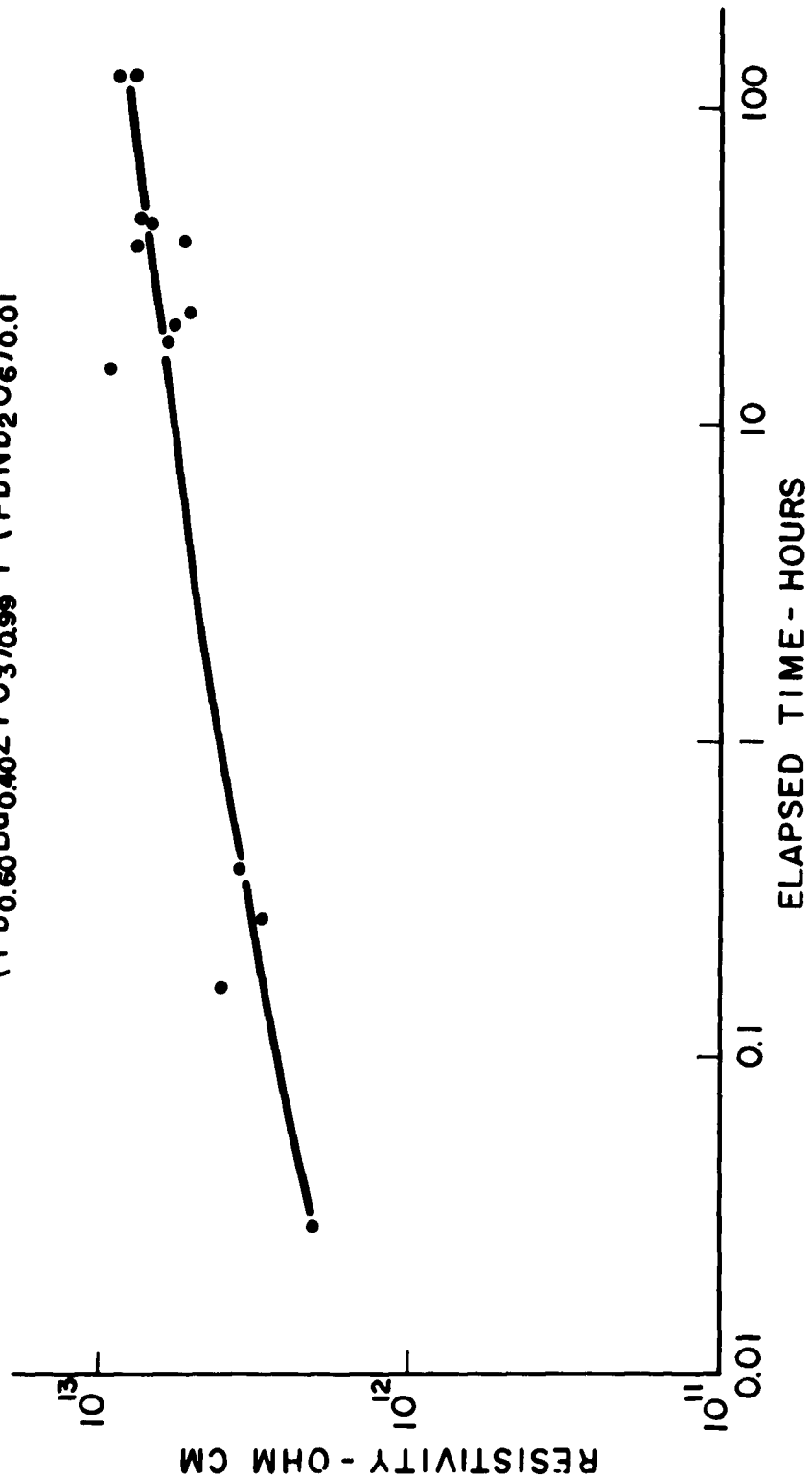


FIGURE 6.
RESISTIVITY VS. ELAPSED TIME
10 KV/CM 230°C
(Pb_{0.50}Sr_{0.50}ZrO₃)_{0.99} + (PbNb₂O₆)_{0.01}

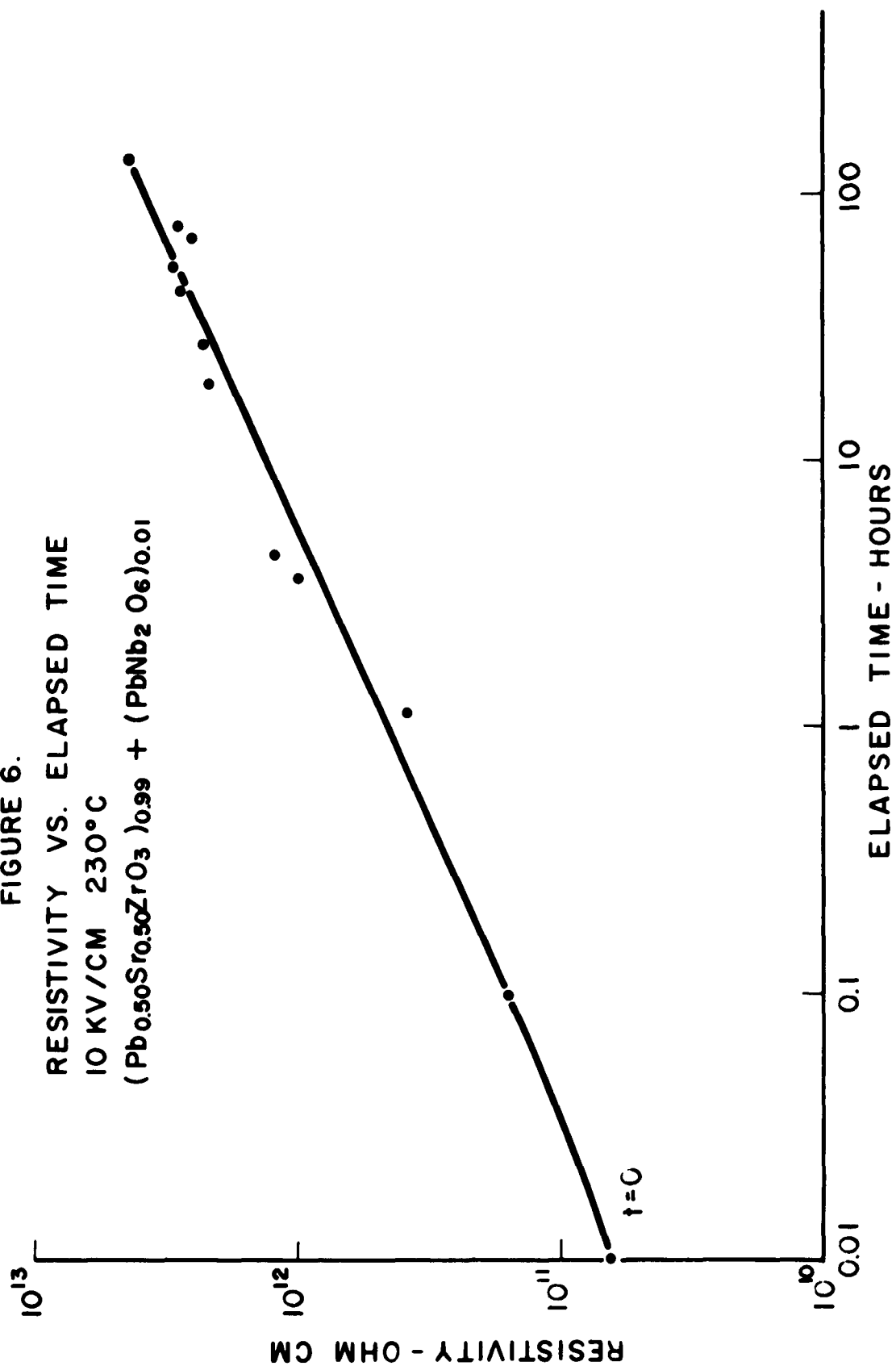


FIGURE 7.
 RESISTIVITY VS. ELAPSED TIME
 AVERAGE CURVE FOR THREE SAMPLES
 10 KV/CM 230°C
 $(\text{Pb}_{0.30}\text{Sr}_{0.70}\text{TiO}_3)_{0.99} + (\text{PbNb}_2\text{O}_6)_{0.01}$

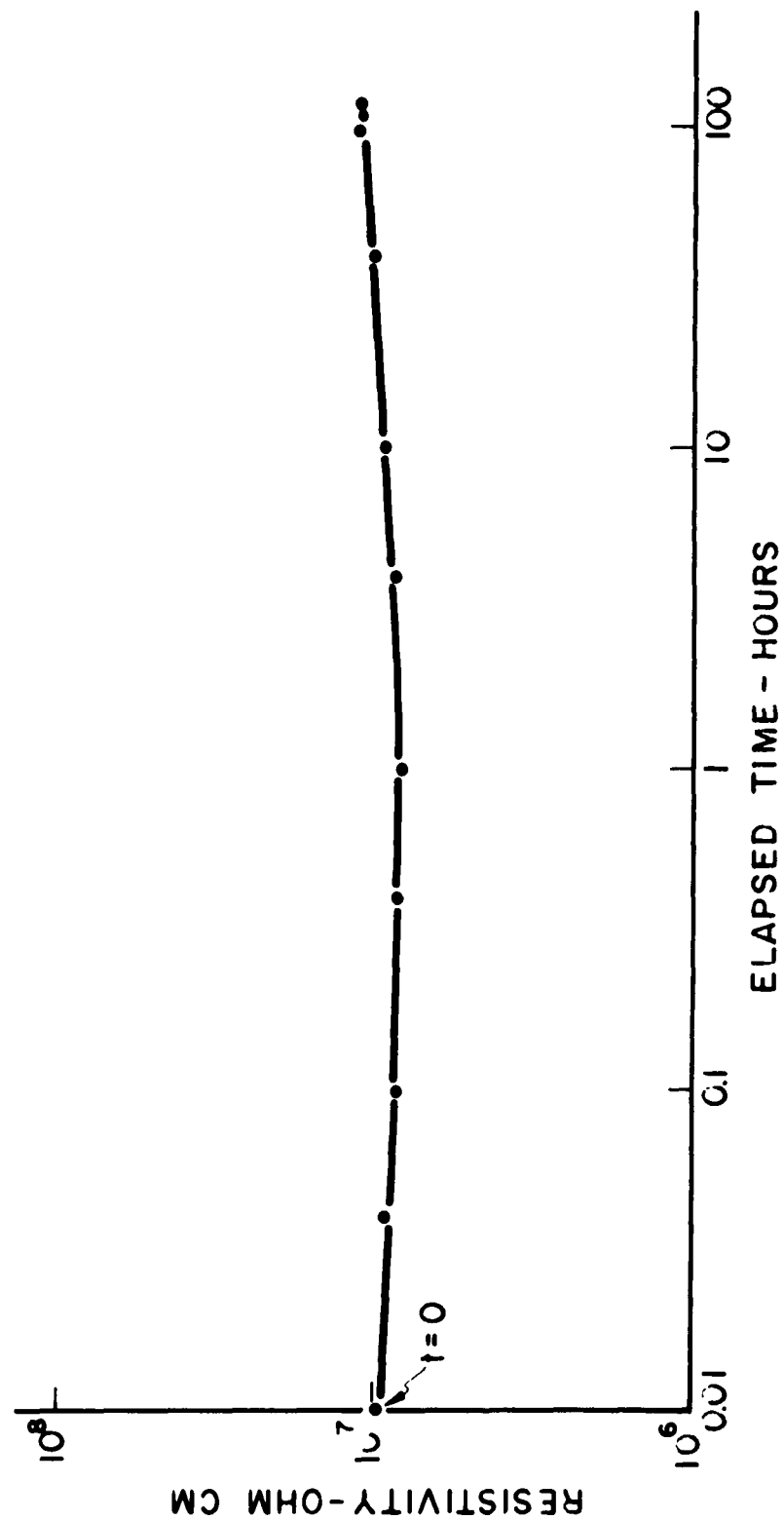


FIGURE 8.
RESISTIVITY VS. ELAPSED TIME
AVERAGE CURVE FOR 3 SAMPLES
10 KV/CM 230°C
 $\text{Pb}_{0.30}\text{Sr}_{0.70}\text{TiO}_3$

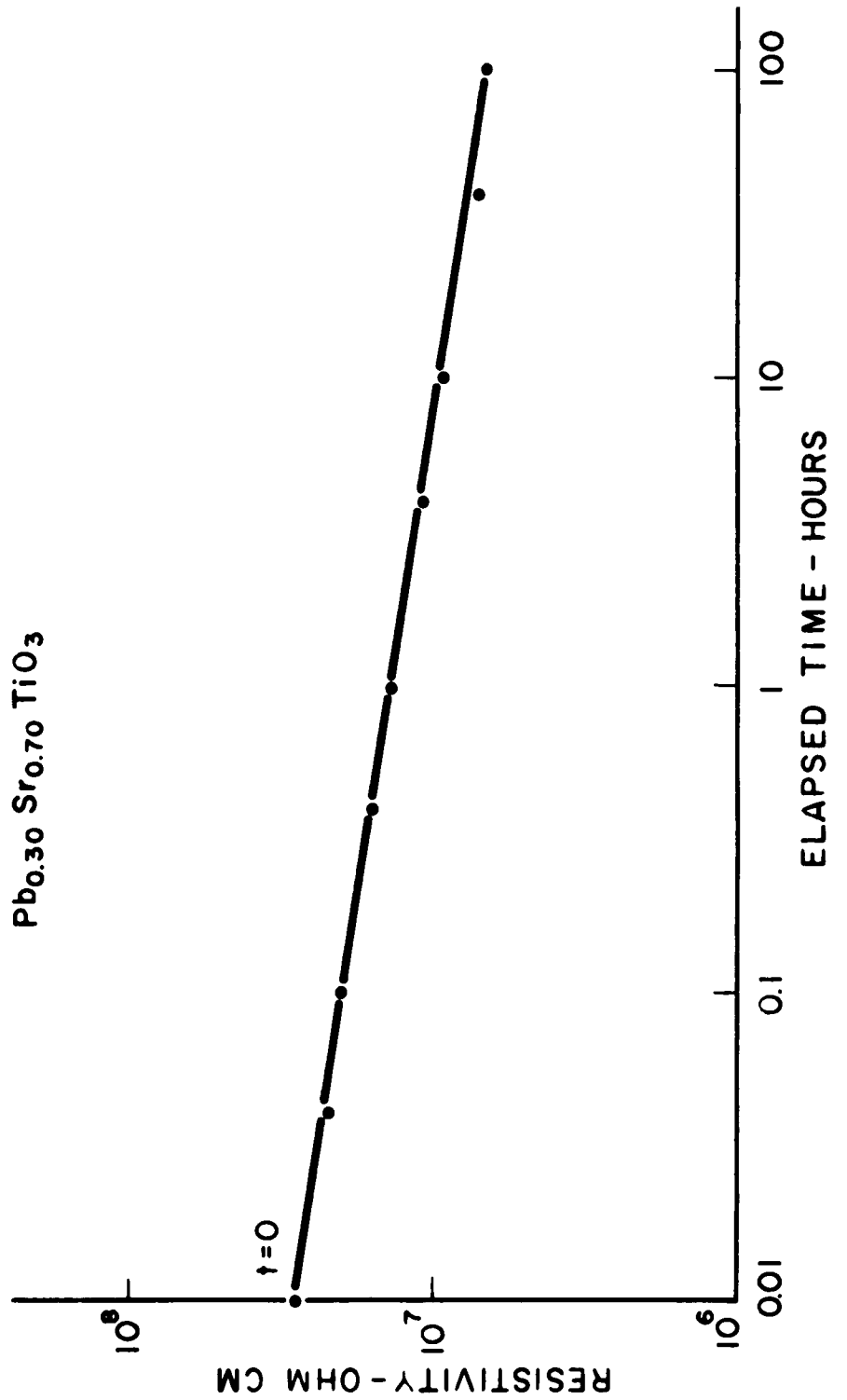


FIGURE 9.
RESISTIVITY VS. ELAPSED TIME.
AVERAGE CURVE FOR 3 SAMPLES
10 KV/CM 230°C
 $(\text{Pb}_{0.50}\text{Sr}_{0.50}\text{TiO}_3)_{0.99} + (\text{PbNb}_2\text{O}_6)_{0.01}$

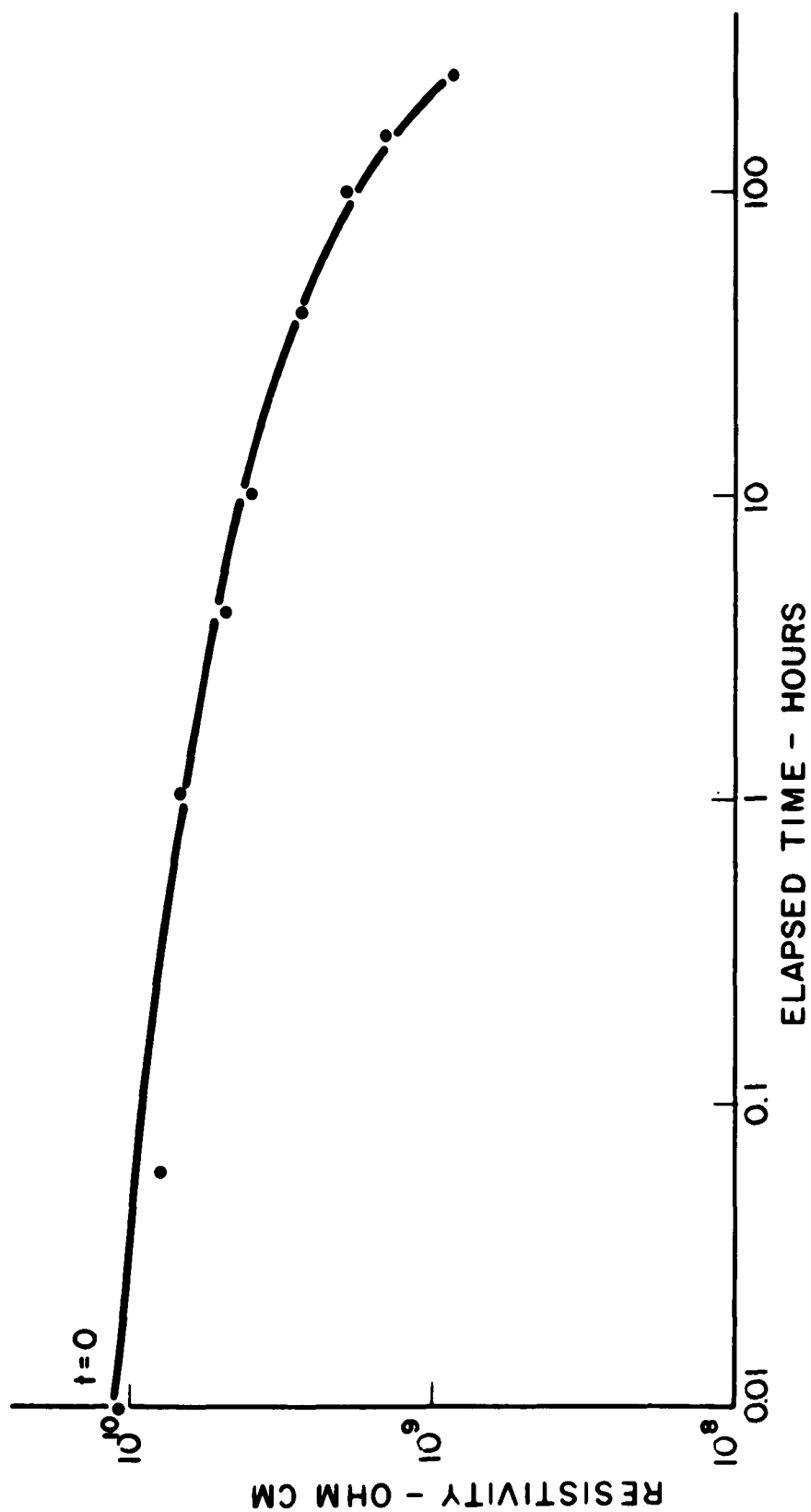


FIGURE 10.
RESISTIVITY VS. ELAPSED TIME
10 KV/CM 230°C
 $(\text{Pb}_{0.30}\text{Sr}_{0.70}\text{TiO}_3)_{0.99} + (\text{Pb}_2\text{Sc}_2\text{O}_5)_{0.01}$

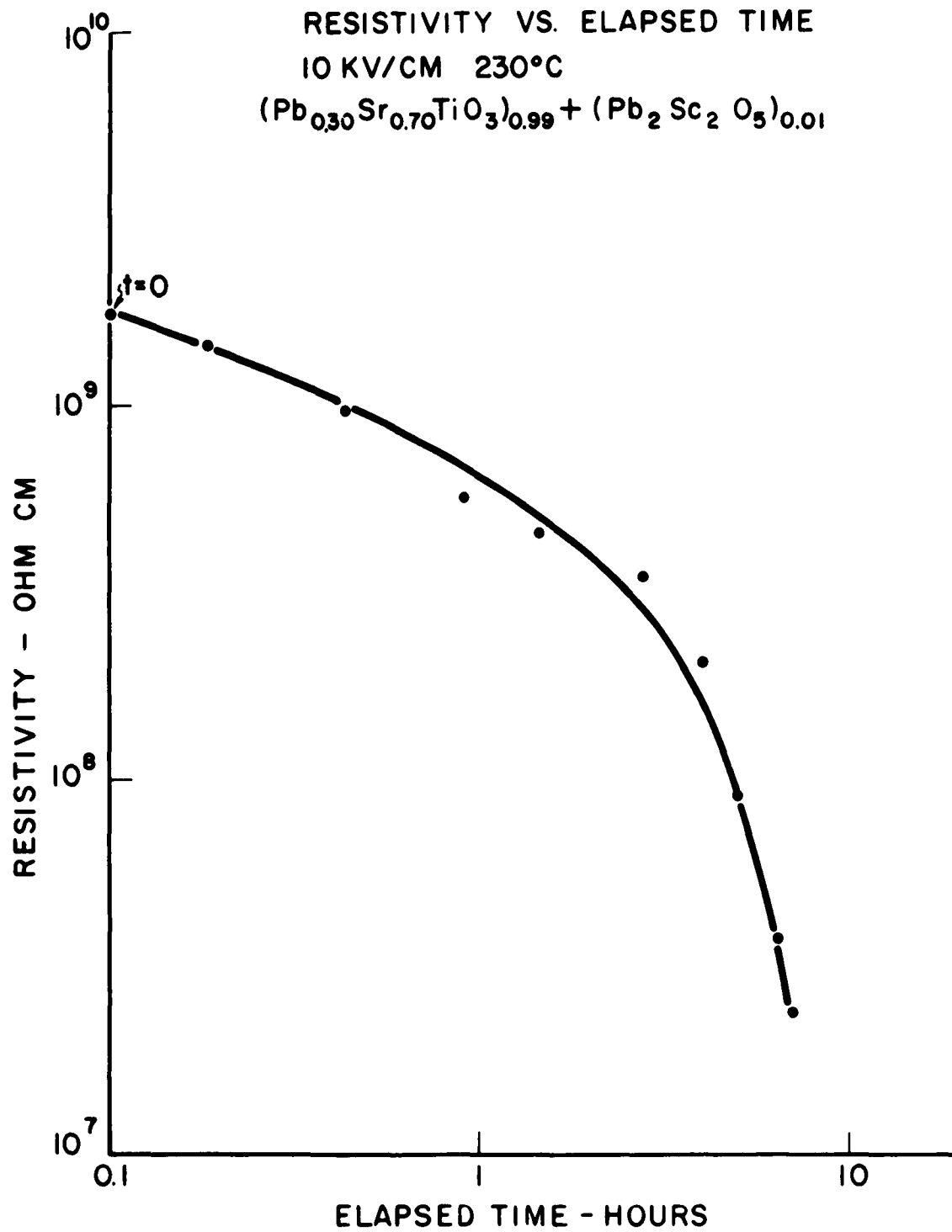


Table I. Classification of Compositions with Respect to Their Behavior During Degradation Tests

| Composition | ρ after/ ρ before 10kV/cm, 230°C | ϵ/ϵ_0 at 1 mc, $\tan \delta$ at 1 mc, ϵ/ϵ_0 at 230°C 25°C | | ρ (230°C, 10KV/cm) Before life test | Grain Size Microns | | | |
|---|---|--|---------------|---|-----------------------|---------------|------------------------|-----------|
| | | Before | After | | | | | |
| (PbZrO ₃) _{0.98} + (PbNb ₂ O ₆) _{0.02} | 78 | 590 (1kc) | 510 (1kc) | 0.032 (1kc) | 0.030 (1kc) | 3375 (1kc) | 6 x 10 ⁹ | < 1 to 2 |
| (Pb _{0.50} Sr _{0.50} ZrO ₃) _{0.99} ⁺ (PbNb ₂ O ₆) _{0.01} | 69 | 166 (1kc) | 170 (1kc) | --- | --- | 121 | 6.2 x 10 ¹⁰ | 10 to 25 |
| PbZrO ₃ | 18 | 169 (1kc) | 134 (1kc) | 0.0031 (1kc) | 0.0056 (1kc) | 4800 (1kc) | 3.4 x 10 ⁸ | < 1 to 6 |
| Pb _{0.60} Ba _{0.40} ZrO ₃ | 13 | 3560 | 1510 | 0.040 | 0.034 | 1060 | 1.1 x 10 ⁸ | < 1 to 6 |
| (Pb _{0.60} Ba _{0.40} ZrO ₃) _{0.99} ⁺ (PbNb ₂ O ₆) _{0.01} | 3.8 | 3712 | 2425 | 0.02 | 0.0038 | 700 | 2.0 x 10 ¹² | 5 - 25 |
| (Pb _{0.30} Sr _{0.70} TiO ₃) _{0.99} ⁺ (PbNb ₂ O ₆) _{0.01} | 1.2 | 4950 | 5840 | 0.062 | 0.017 | 1500 | 9.8 x 10 ⁶ | < 1 to 3 |
| Pb _{0.30} Sr _{0.70} TiO ₃ | 0.23 | 2880 (1kc) | 2650 (1kc) | 0.012 (1kc) | 0.024 (1kc) | 400 | 2.9 x 10 ⁷ | 5 to 15 |
| (Pb _{0.50} Sr _{0.50} TiO ₃) _{0.99} ⁺ (PbNb ₂ O ₆) _{0.01} | 0.08 | 1150 | 763 | 0.030 | 0.021 | 1450 | 1.1 x 10 ¹⁰ | 1 to 10 |
| (Pb _{0.30} Sr _{0.70} TiO ₃) _{0.99} ⁺ (Pb ₂ Sc ₂ O ₅) _{0.01} | 0.016 | 1100 | --- | 0.014 | --- | 500 | 1.7 x 10 ⁹ | 3 (max.) |

ratio of volume resistivity after life test to before life test measured at 230°C with electric field maintained at 10 kv/cm. The table also lists values of ϵ/ϵ_0 and $\tan \delta$ before and after the life test measured at 25°C and one mcps with an electric field of about 1 volt/mm.

Behavior of the zirconates and titanates is quite different, the former all increasing in resistivity during the life test here described, the latter generally decreasing. Behavior with respect to changes in $\tan \delta$ and dielectric constant are not correlated so neatly. One would expect degradation to be less severe with materials having high initial values of volume resistivity, but this has not followed consistently in this work. One might also expect dielectric degradation to be most severe with high dielectric constant materials, and this is generally true. There are some exceptions in this work, however (Table I).

One is, of course, concerned not only with the overall effects of the life test on the volume resistivity and dielectric constant, but also with the actual final values. For instance, the volume resistivity of $\text{Pb}_{0.60}\text{Ba}_{0.40}\text{ZrO}_3$ increased by a factor of 12 compared to an increase of only 4 for the same composition with Nb^{5+} . The final value for the latter, however, was over three orders of magnitude higher than that of the former.

On the basis of relatively little evidence so far it appears that 2 atom % Sc^{3+} in the B-position of $\text{Pb}_{0.50}\text{Sr}_{0.50}\text{TiO}_3$ speeds the degradation process, while 2 atom % Nb^{5+} also in the B-position inhibits the process. In the latter case, however, it appears that the initial value was anomalously low. At low electric field the 230°C value of the volume resistivity for this composition is about 100 times higher (Figure 2, Quarterly Technical Note No. 2).

Probably the most remarkable composition studied to this point is $\text{Pb}_{0.60}\text{Ba}_{0.40}\text{ZrO}_3$ with 2 atom % Nb^{5+} . Here the initial and final values of volume resistivity measured at 230°C with an electric field 10 kv/cm were 2×10^{12} and 8×10^{12} ohm cm respectively. The time constant ($\rho \epsilon$) after the life test was 400 seconds at 230°C.

It is, of course, clear that improvement in volume resistivity under high dc electric fields will not continue indefinitely. The data in Figures 3 through 5 indicate a tendency toward saturation, but it appears that the time necessary may

be more than 1000 hours. It is not possible at this time to predict behavior after saturation; there may be a gradual but accelerating degradation, or degradation may come very rapidly. The data in Figures 9 and 10, obtained on titanates suffering degradation from the very beginning of the tests, indicate an accelerating degradation. The composition with Sc^{3+} (Figure 10) was very close to failure after only seven hours.

Lehovec and Shirn⁽⁴⁾ studied degradation of barium titanate with sufficient calcium zirconate to reduce the Curie point to about 35°C. They found that at temperatures between 250 and 300°C and with electric field in the range 2 to 6 kv/cm the current increased initially, decreased for a time, and then increased again. They studied the potential distribution during this period and concluded that there was first injection of a high conductivity region from the cathode and then injection of a low conductivity region from the anode. They postulated that this low conductivity region traveled to the cathode, and that the resulting high electric field at the cathode caused renewed injection of high conductivity from the cathode.

In this work results have not in general been similar to those of Lehovec and Shirn. It is possible that this may be due at least partly to use of a different electrode material, gold in this work and Aquadag in the work of reference (4). The geometry of test specimens was also quite different, with end-electroded bars used in the work of reference (4).

In another respect this work and that of reference (4) are in agreement. It was noted in reference (4) that the layers of different resistivity have characteristic color differences, and these color differences have been noted also in this work. In the work of reference (4) it was postulated that the high conductivity region is related not only to injection of electrons at the cathode, but also to an increase in oxygen vacancies.

An attempt was made to correlate the photomicrographs shown in Quarterly Technical Note No. 2 with behavior summarized in Figures 3 through 10 and Table I. Ranges of grain sizes are listed in Table I, and it is readily noted that there is apparently no correlation. The best composition tested to

(4) K. Lehovec and G. A. Shirn, J. Appl. Phys. 33, 2036 (1962).

date, $\text{Pb}_{0.60}\text{Ba}_{0.40}\text{ZrO}_3$ with 2 atom % Nb^{5+} , has a fairly high proportion of very large grains and relatively small grains (Figure 16 of Quarterly Technical Note No. 2), however, and this may be significant.

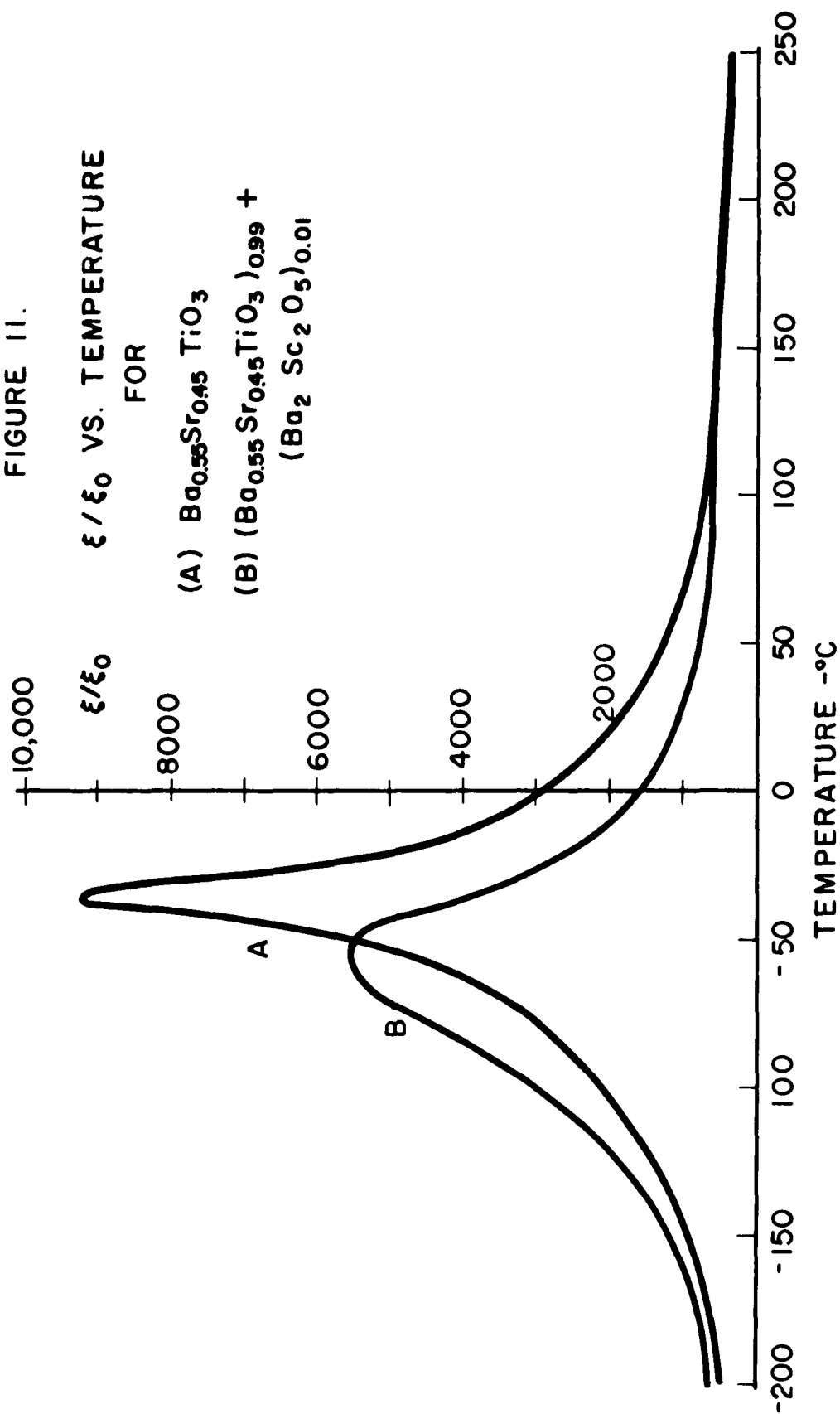
II. PERMITTIVITY-TEMPERATURE CURVES

Permittivity-temperature curves prepared during this period are shown in Figures 11 through 13. It may be of some interest to note that PbZrO_3 with 2 atom % Nb^{5+} has a peak permittivity of about 10,000 and it is ferroelectric just below the Curie point. Plain PbZrO_3 has a peak permittivity of about 6,000 (Figure 4 of Quarterly Technical Note No. 1), and it is antiferroelectric just below the Curie point. With Sc^{3+} the peak permittivity is only 3300, indicating that Sc^{3+} in place of Zr^{4+} encourages antiferroelectricity; i. e., with Sc^{3+} the difference in free energy between the ferroelectric and antiferroelectric states is increased.

III. FUTURE PLANS

Degradation studies will be continued and extended to include different compositions. For promising materials the tests may be continued to longer periods, and tests may be repeated at several temperatures. Further attempts will be made to correlate other physical properties to results of the degradation studies.

FIGURE 11.



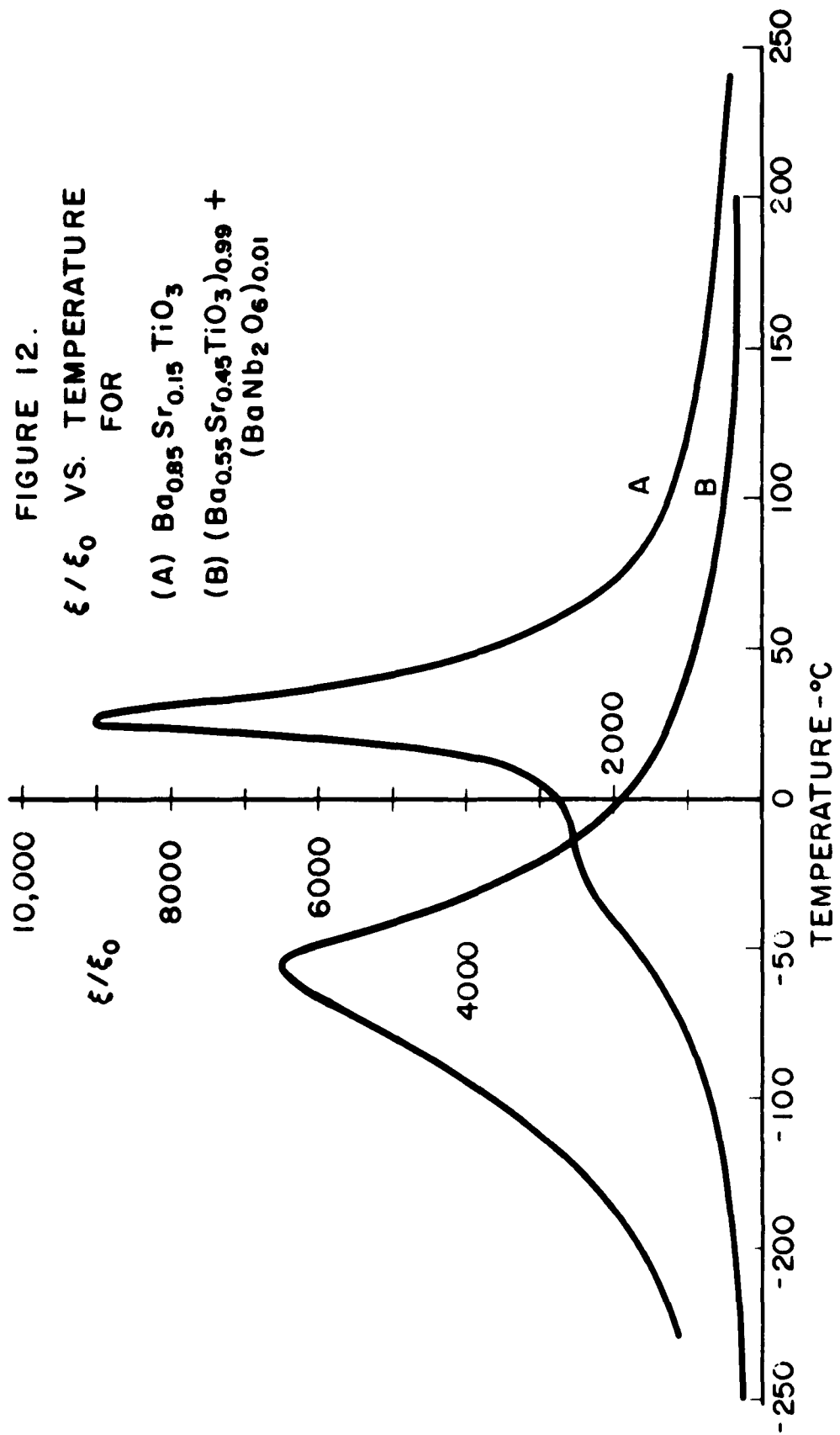
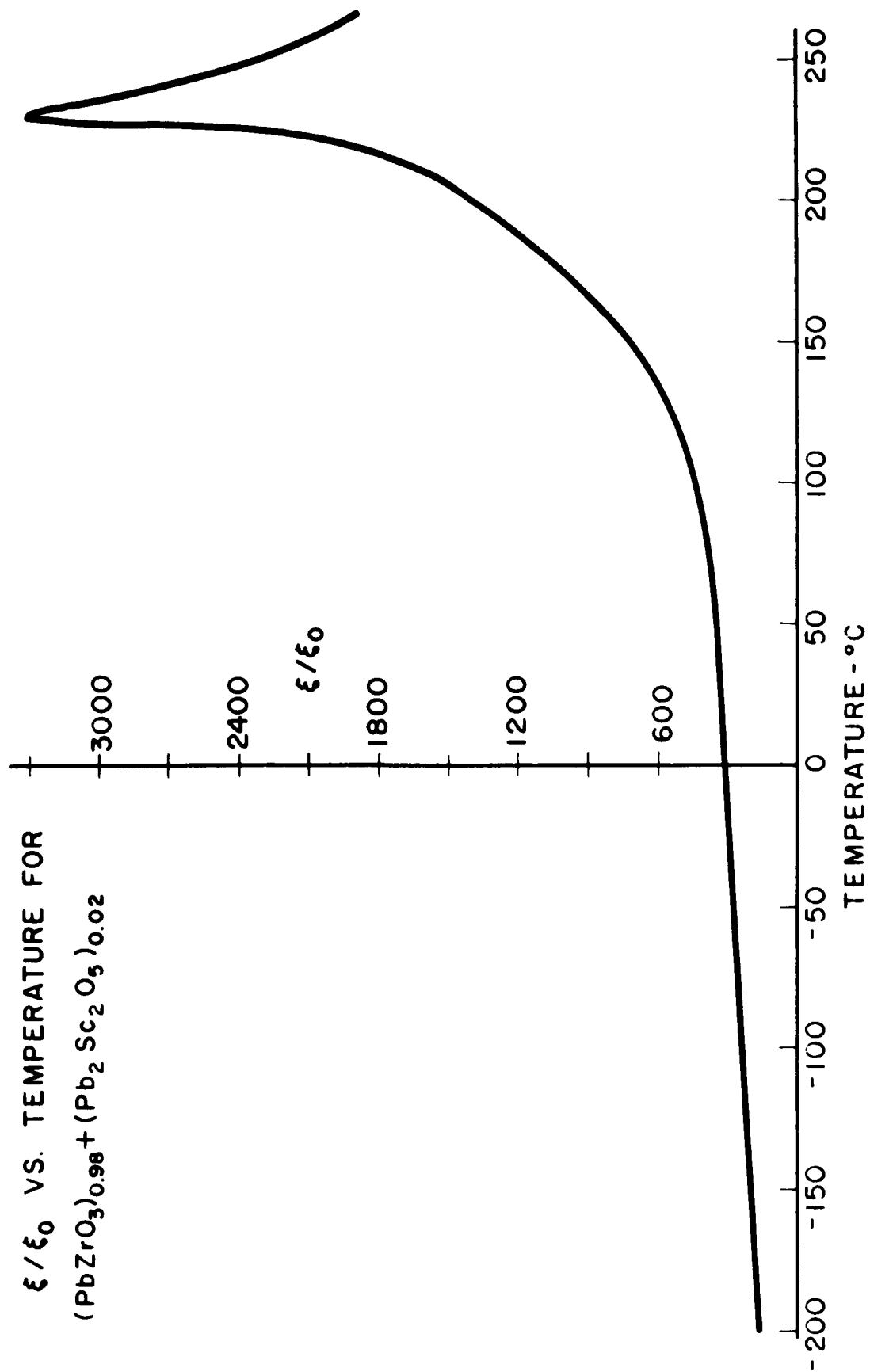


FIGURE 13.
 ξ / ξ_0 VS. TEMPERATURE FOR
 $(\text{PbZrO}_3)_{0.98} + (\text{Pb}_2\text{Sc}_2\text{O}_5)_{0.02}$



INITIAL DISTRIBUTION

Copy No.

| | |
|---------|---|
| 1 | Electronic Research Division (H. Jaffe) |
| 2 | Electronic Research Division (Don A. Berlincourt) |
| 3 | Clevite Patent Department |
| 4-9 | Clevite Library |
| 10 | Electronic Research Division (Project Administration) |
| 11 | Electronic Research Division (B. Jaffe) |
| 12 | Electronic Research Division (J. Koenig) |
| 13 | Electronic Research Division (F. Kulcsar) |
| 14 | Electronic Research Division (J. Peterson) |
| 15-114 | RADC Distribution List |
| 115-120 | Electronic Research Division |

DISTRIBUTION LIST FOR CONTRACT REPORTS

Contract No. AF 30(602)-2594

Electronic Research Division
Clevite Corporation

| | <u>No. Copies</u> |
|---|-------------------|
| RADC (RASGP, Attn: E. A. Doyle, Jr.) Griffiss Air Force Base, New York | 1 |
| RADC (RAAPT) Griffiss Air Force Base, New York | 1 |
| RADC (RAALD) Griffiss Air Force Base, New York | 1 |
| GEEIA (ROZMCAT) Griffiss Air Force Base, New York | 1 |
| RADC (RAIS, Attn: Mr. Malloy) Griffiss Air Force Base, New York | 1 |
| U. S. Army Electronics R&D Laboratories Liaison Officer RADC Griffiss Air Force Base, New York | 1 |
| AUL (3T) Maxwell Air Force Base, Alabama | 1 |
| ASD (ASAPRD) Wright-Patterson Air Force Base, Ohio | 1 |
| Chief, Naval Research Laboratory Attn: Code 2027 Washington 25, D. C. | 1 |
| Air Force Field Representative Naval Research Laboratory Attn: Code 1010 Washington 25, D. C. | 1 |
| Commanding Officer U. S. Army Electronics R&D Laboratories Attn: SELRA/SL-ADT Ft. Monmouth, New Jersey | 1 |

DISTRIBUTION LIST FOR CONTRACT REPORTS

Contract No. AF 30(602)-2594

| | <u>No. Copies</u> |
|--|-------------------|
| National Aeronautics & Space Administration Langley Research Center Langley Station Hampton, Virginia Attention: Librarian | 1 |
| Bell & Howell Research Center Attn: R. L. Brownell 360 Sierra Madre Villa Pasadena, California | 1 |
| Central Intelligence Agency Attn: OCR Mail Room 2430 E. Street N. W. Washington 25, D. C. | 1 |
| US Strike Command Attn: STRJ5-OR MacDill Air Force Base, Florida | 1 |
| AFSC (SCSE) Andrews Air Force Base Washington 25, D. C. | 1 |
| Commanding General U. S. Army Electronic Proving Ground Attn: Technical Documents Library Ft. Huachuca, Arizona | 1 |
| ASTIA (TISIA-2) Arlington Hall Station Arlington 12, Virginia | 10 |
| AFSC (SCFRE) Andrews Air Force Base, Washington 25, D. C. | 1 |
| Headquarters USAF (AFCOA) Washington 25, D. C. | 1 |
| AFOSR (SRAS/Dr. G. R. Eber) Holloman Air Force Base, New Mexico | 1 |

DISTRIBUTION LIST FOR CONTRACT REPORTS

Contract No. AF 30(602)-2594

| | <u>No. Copies</u> |
|--|-------------------|
| Office of Chief of Naval Operations (Op-724) Navy Department Washington 25, D. C. | 1 |
| Commander U. S. Naval Air Development Center (NADC Lib) Johnsville, Pennsylvania | 1 |
| Commander Naval Missile Center Technical Library (Code NO 3022) Pt. Mugu, California | 1 |
| Bureau of Naval Weapons Main Navy Building Washington 25, D. C. Attn: Technical Librarian, DL1-3 | 1 |
| Redstone Scientific Information Center U. S. Army Missile Command Redstone Arsenal, Alabama Attn: Technical Library | 1 |
| Commandant Armed Forces Staff College (Library) Norfolk 11, Virginia | 1 |
| ADC (ADOAC-DL) Ent Air Force Base, Colorado | 1 |
| AFFTC (FTOOT) Edwards Air Force Base, California | 1 |
| Commander U. S. Naval Ordnance Laboratory (Technical Library) White Oak, Silver Springs, Maryland | 1 |
| Commanding General White Sands Missile Range New Mexico Attn: Technical Library | 1 |

DISTRIBUTION LIST FOR CONTRACT REPORTS

Contract No. AF 30(602)-2594

| | <u>No. Copies</u> |
|---|-------------------|
| Director U. S. Army Engineer R&D Laboratories Technical Documents Center Ft. Belvoir, Virginia | 1 |
| ESD (ESRL) L. G. Hanscom Field Bedford, Massachusetts | 1 |
| Commanding Officer & Director U. S. Navy Electronics Laboratory (LIB) San Diego 52, California | 1 |
| ESD (ESAT) L. G. Hanscom Field Bedford, Massachusetts | 1 |
| Commandant U. S. Army War College (Library) Carlisle Barracks, Pennsylvania | 1 |
| APGC (PGAPI) Eglin Air Force Base, Florida | 1 |
| AFSWC (SWOI) Kirtland Air Force Base, New Mexico | 1 |
| AFMTC (Technical Library MU-135) Patrick Air Force Base, Florida | 1 |
| RTD (RTGS) Bolling Air Force Base, Washington 25, D. C. | 1 |
| ESD (ESGT) L. G. Hanscom Field Bedford, Massachusetts | 2 |
| ESD (ESRDE, Major James W. Van Horn) L. G. Hanscom Field Bedford, Massachusetts | 1 |

DISTRIBUTION LIST FOR CONTRACT REPORTS

Contract No. AF 30(602)-2594

| | <u>No. Copies</u> |
|--|-------------------|
| ASD (ASRCTE, Mr. E. Miller) Wright-Patterson Air Force Base, Ohio | 1 |
| Westinghouse Electric Corporation Air Arm Division (Dr. John Dzimianski) Friendship International Airport P. O. Box 1897 Baltimore 3, Maryland | 2 |
| Motorola, Inc. Solid State Integrated Circuits Laboratory Attn: Mr. J. R. Black 8201 E. McDowell Road Scottsdale, Arizona | 2 |
| Hughes Aircraft Company Ground Systems Division Attn: Mr. F. M. LaFleur Fullerton, California | 2 |
| Dr. Robert Gerson Department of Physics University of Missouri School of Mines & Metallurgy Rolla, Missouri | |
| Armour Research Foundation Illinois Institute of Technology Technology Center Attn: Dr. G. T. Jacobi Chicago 16, Illinois | 2 |
| Raytheon Company Research Division Attn: Dr. P. Nutter Waltham 54, Massachusetts | 2 |
| General Telephone and Electric Bayside Laboratories Attn: Dr. Thomas Polanyi Bayside, New York | 2 |

DISTRIBUTION LIST FOR CONTRACT REPORTS

Contract No. AF 30(602)-2594

| | <u>No. Copies</u> |
|---|-------------------|
| Syracuse University Attn: Dr. Glen Glasford Syracuse, New York | 2 |
| Clevite Corporation Shockley Transistor Division Attn: Dr. Hans Queisser Stanford Industrial Park Palo Alto, California | 2 |
| Sprague Electric Company Attn: Dr. Preston Robinson Director, Consultant N. Adams, Massachusetts | 1 |
| Frank Brand Chief Microwave Quantum Electronics Br. SIGRA/SL-PFM Ft. Monmouth, New Jersey | 1 |
| William Spurgeon Bendix Corporation Research Laboratory Division Southfield, Michigan | 1 |
| Autonetics Division, North American Attn: Dr. West 9150 E. Imperial Highway Downey, California | 1 |
| John G. Landers 307 The Great Road Bedford, Massachusetts | 1 |
| Internation Resistance Company Attn: Jack Iskind Project Manager XTL Resistors 401 N. Broad Street Philadelphia, Pennsylvania | 1 |

DISTRIBUTION LIST FOR CONTRACT REPORTS

Contract No. AF 30(602)-2594

| | <u>No. Copies</u> |
|--|-------------------|
| Avco, RAD Attn: Mr. D. Earles 201 Lowell Street Wilmington, Massachusetts | 1 |
| Commanding Officer Diamond Ordnance Fuse Laboratories Attn: Mr. Asaf A. Benderly Washington 25, D. C. | 1 |
| Corning Glass Works Electronic Components Division Attn: Mr. Richard O'Brien Bradford, Pennsylvania | 1 |
| Fairchild Semiconductor Corporation Attn: Mr. Jack Gorry 545 Whisman Road Mountainview, California | 1 |
| General Electric Company Semiconductor Products Department Attn: Mr. Conrad Zierat Electronics Park Syracuse, New York | 1 |
| Pacific Semiconductor, Inc. Attn: Mr. R. A. Campbell Culver City, California | 1 |
| Minneapolis Honeywell Attn: Mr. J. M. Bedrick 1400 Soldiers Field Road Boston, Massachusetts | 1 |
| General Telephone and Electronics Laboratories Attn: Mr. Daniel George Bayside, New York | 2 |
| USASRDL (SIGRA/SL-PFS, Mr. N. Korolkoff) Evans Area, Ft. Monmouth, New Jersey | 2 |

DISTRIBUTION LIST FOR CONTRACT REPORTS

Contract No. AF 30(602)-2594

| | <u>No. Copies</u> |
|--|-------------------|
| AGED Secretariat Working Group on Low Power Devices 346 Broadway New York 13, New York | 3 |
| Texas Instruments, Inc. Attn: Semiconductor Components Library P. O. Box 5012 Dallas 22, Texas | 1 |
| Microwave Associates, Inc. Attn: Dr. Arthur Uhler, Jr. Burlington, Massachusetts | 1 |
| Motorola, Inc. Semiconductor Products Division Attn: Dr. Steward S. Flaschen 5005 E. McDowell Road Phoenix, Arizona | 2 |
| General Electric Company Valley Forge Technology Center Attn: Mr. T. G. Nicoforo P. O. Box 8555 Philadelphia 1, Pennsylvania | 1 |
| Battelle Memorial Institute Attn: Mr. T. Schilladay Columbus, Ohio | 1 |